Field sensing characteristics of magnetic tunnel junctions with (001) MgO tunnel barrier

Dipanjan Mazumdar,[1,a)] Weifeng Shen,[1] Xiaoyong Liu,[1,2] B. D. Schrag,[1,2] Matthew Carter,[1,2] and Gang Xiao[1]
[1]*Physics Department, Brown University, 182 Hope St., Providence, Rhode Island 02912, USA*
[2]*Micro Magnetics Inc., 421 Currant Road, Fall River, Massachusetts 02720, USA*

(Received 19 January 2008; accepted 9 April 2008; published online 10 June 2008)

We map the magnetic field sensitivity and low-frequency $1/f$ voltage noise of high magnetoresistance MgO-based magnetic tunnel junctions in an orthogonal magnetic field arrangement. Large sensitivity values of over 1%/Oe are obtained only when a sufficiently large hard-axis bias field is applied. The low-frequency voltage noise is observed to scale with the field sensitivity. The magnetic field noise map reveals that the signal-to-noise ratios of these devices get gradually better at higher hard-axis bias fields. © *2008 American Institute of Physics*. [DOI: 10.1063/1.2939265]

I. INTRODUCTION

Successful realization of spin-coherent tunneling in (001) MgO-based magnetic tunnel junctions (MTJs) has pushed the tunnel magnetoresistance (TMR) values to well beyond 100%.[1,2] Due to the selective filtering effects of the MgO tunnel barrier on the $3d$ wavefunction, conventional ferromagnets or their alloys can be used as the ferromagnetic electrode to achieve high spin polarization and large TMR ratios.[3,4]

MgO-based MTJs have enormous potential in low-field sensing applications. For a proper characterization of the field sensing properties of these devices, simultaneous investigations into the magnetic field sensitivity and low-frequency voltage noise characteristics are absolutely essential. Field sensitivity depends crucially on the magnetic properties of the MTJ free layer in addition to the magnitude of the TMR effect. Low-frequency voltage noise in MTJs is usually dominated by a $1/f$ noise spectrum, which arises from either charge traps within the MgO barrier or from fluctuations in the magnetization of the free layer.[5–8] In this work, we investigate the performance of MgO-MTJs by mapping their magnetic field sensitivity and low-frequency noise in an orthogonal magnetic field arrangement. Our sensitivity analysis show that sensitivities in excess of 1%/Oe is achieved only when a sufficiently strong hard-axis bias field is applied, but the maximum sensitivity is not obtained at zero field due to magnetic coupling of the free layer and the pinned layer. Our noise investigations show that the magnetic field noise of the MTJ device is lower at higher hard-axis bias fields, improving the magnetic field sensing characteristics of MgO-MTJs.

The magnetic field sensitivity is defined as

$$s = 1/V(dV/dH) = 1/R(dR/dH), \tag{1}$$

and the magnetic field noise is obtained by dividing the normalized voltage noise by the field sensitivity,

$$S_H = (S_v^{0.5}/V)/s = (\delta V/V)/s, \tag{2}$$

where S_v is the power spectral density, δV is the voltage noise, V is the electrical bias voltage, and R is the device resistance. Magnetic field noise can be conveniently expressed in terms of $\mathrm{nT/Hz^{0.5}}$ and *normalized* voltage noise in units of $\mathrm{Hz^{-0.5}}$.

II. EXPERIMENT

Micron-sized MTJ spin valves with $Ni_{79}Fe_{21}$ free layer were prepared using magnetron sputtering on thermally oxidized Si wafers with the following structure (units in angstrom): Ta(300) / $Co_{50}Fe_{50}$(20) / IrMn(150) / $Co_{40}Fe_{50}$(20) / Ru(8) / $Co_{40}Fe_{40}B_{20}$(30) / MgO(16) / $Ni_{79}Fe_{21}$(30) / Ta(100) / Ru(50). A schematic diagram of our full structure is shown in Fig. 1(a). Details of our sample fabrication methods are reported elsewhere.[9] The magnetoresistance (MR) response of a typical MgO-MTJ sample in the optimal sensing configuration is shown in Fig. 1(b), where a hard-axis bias field of 50 Oe is applied. A MR of over 100% with excellent exchange bias properties was observed in all our samples. The residual hysteresis in the MR loop of Fig. 1(b) is from the magnetic circuit of our experimental setup and not a feature of the MTJ.

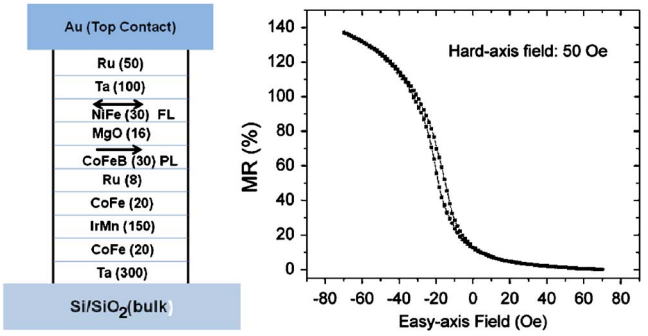

FIG. 1. (Color online) (a) The full MTJ structure used for the fabrication of high TMR MTJs with NiFe free layer and CoFeB pinned layer. (b) The full MR response of a typical MgO-MTJ sample when a hard-axis bias field of 50 Oe is applied.

[a)]Electronic mail: dmazumdar@mint.ua.edu.

Both sensitivity and noise measurements were performed in an identical arrangement of orthogonal magnetic fields applied along the easy (H_E) and hard (H_B) axes of the MTJ. In the sensitivity-map setup, a pair of Helmholtz coils generated a small ac field ($\Delta H \sim 1$ Oe) along the easy axis of the MTJ. The output ac voltage ΔV, in response to ΔH, was then measured by a lock-in amplifier as a function of H_E and H_B.

Noise measurements were performed in an electrostatically shielded box to suppress spurious environmental noise sources. The four-lead MTJ device was mounted on a custom-made printed circuit board equipped with two low-noise preamplifiers and the amplified noise voltage was fed to an HP-35760A spectrum analyzer operating in cross-correlation mode. The junctions were biased to a relatively high voltage (200 mV) and data measured from 1 Hz to 51.2 kHz. The custom-made noise board was designed to fit the small air gap of the cross-paired electromagnets.

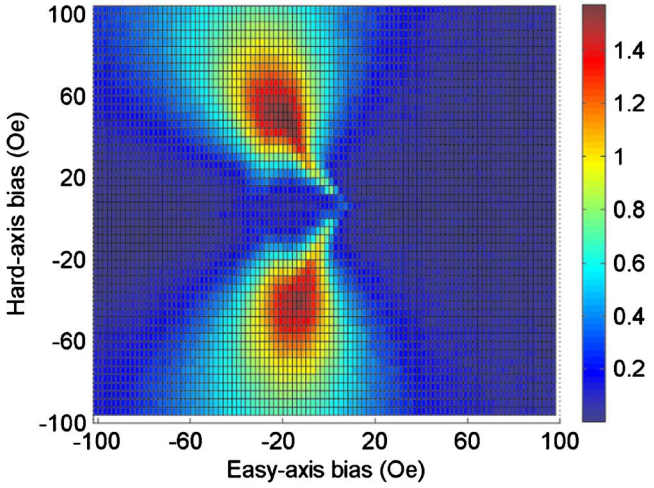

FIG. 2. (Color online) Magnetic field sensitivity of a typical MgO-MTJ plotted in units of%/Oe as a function of orthogonal easy- and hard-axis bias fields (the sensitivity map). Two high sensitivity spots are observed with highest values of almost 1.5%/Oe centered at $|H_B| \sim H_K = 50$ Oe and $H_E \sim -20$ Oe. The shift of the maximum from the $H_E = 0$ Oe axis is predominantly due to Neel coupling between the free and pinned layers.

III. RESULTS AND DISCUSSIONS

The MTJ response is highly nonlinear and hysteretic without the application of a hard-axis bias field, therefore unsuitable for any field sensing purposes. In such a case, the free layer switches completely over a very small dynamic field range, and the hysteretic nature makes the response irreversible. In other words, the field sensitivity in the absense of an external hard bias field [Eq. (1)] is negligibly small, even though the MR response is nominally over 100%. However, the application of a hard-axis bias field gradually overcomes the energy barrier that prevents the free layer from switching and over a certain hard-axis bias field, called the anisotropy field (H_K), the free layer response is completely reversible and nonhysteretic. In this case, the free layer is said to rotate coherently, always in the resultant field direction.

Assuming that the free layer is nonhysteretic, we rewrite Eq. (1) as

$$1/R(dR/dH) = 1/R(dR/d\theta)(d\theta/dH). \tag{3}$$

The magnetization direction approximately changes by π when the external field changes by $\sim 2H_K$. However, in general, $d\theta/dH \approx \pi/\beta H_K$, where β depends on the strength and direction of the total external magnetic field. Further, knowing that the resistive response agrees reasonably well with a cosine function, $dR/d\theta \approx \Delta R \sin\theta$, where ΔR represents the magnitude of the MR effect. Equation (3) can now be written as

$$(\Delta R/R)\Delta H \approx (\Delta R/R)\sin\theta(\pi/\beta H_k). \tag{4}$$

The above expression shows that in order to obtain a high field sensitivity value, the MTJ device must have (1) a high TMR value, (2) an orthogonal alignment of the free and pinned layer magnetization, and (3) a free layer with anisotropy, i.e., a magnetically "soft" material.

All these features are brought out clearly in the sensitivity map of the MTJ device, a typical map of which is shown in Fig. 2. We observe two high sensitivity spots of over 1%/Oe (orange through dark red), which peak at regions centered around $H_B \sim \pm 50$ Oe and $H_E \sim -20$ Oe. In the region between high sensitivity spots, the sensitivity drops steadily and becomes almost zero for $|H_B| < 20$ Oe due to the hysteretic behavior of the MTJ. In the region beyond these spots (high H_B values), the sensitivity decreases again due to an increase in the factor β in Eq. (4). The orthogonal alignment of the free and the pinned layer is achieved only when a sufficiently strong hard bias field is applied to overcome the anisotropy field of the MTJ, which we measure to be approximately 50 Oe for the sensor shown in Fig. 2. This value is significantly higher than the combined magnetocrystalline and shape anisotropy contribution (about 10–20 Oe). This implies that the free layer when put in an MTJ configuration has significantly different switching properties and can probably be only explained by carefully characterizing the domain structure of the MTJ magnetic layers. Also the centers of the high sensitivity spots are shifted from the zero of the easy-axis field to about −20 Oe [similar to Fig. 1(b)]. This is due to the coupling between the ferromagnetic layers, which can originate from direct magnetostatic dipolar interaction between the free-layer (FL) and pinned-layer (PL) or due to Neel coupling.[10] Given that the synthetic-antiferromagnetic pinned layer reduces the direct magnetostatic interaction, coupling of Neel type is thought to be the major source here. It favors a parallel alignment between the layers and reduces the zero field sensitivity of the MTJ device.

Figures 3(a) and 3(b) show the sensitivity map (in units of %/Oe) and the normalized voltage noise map (at 100 Hz in units of $\mathrm{Hz}^{-0.5}$) of a MgO-MTJ sensor. The frequency was chosen to lie well within the $1/f$ spectrum of our MTJs. Both maps look strikingly similar, implying that the voltage noise scales with the sensitivity of the device is therefore dominated by magnetization fluctuations. This is in agreement with our previous findings and reports on alumina-based MTJs.[7,5,11]

Using the normalized voltage noise and sensitivity data

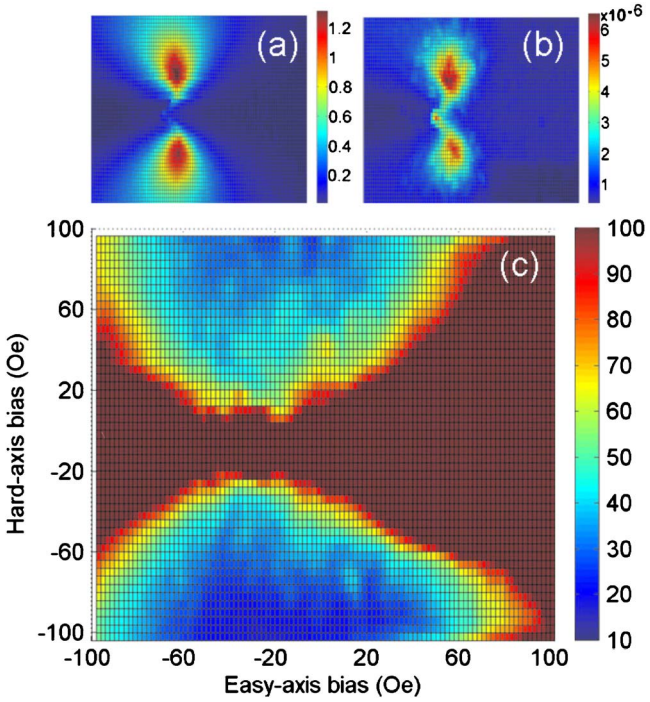

FIG. 3. (Color online) (a) The sensitivity map of a MgO-MTJ (in units of %/Oe) and (b) the corresponding *normalized* voltage noise map in units of $Hz^{-0.5}$, both measured in a 2D orthogonal field arrangement like in Fig. 2. The striking similarity in both maps indicates that the voltage noise is proportional to the field sensitivity. The magnetic FNM is plotted in (c) by dividing the data in (b) by (a), according to Eq. (2). The colorbars are in units of $nT/Hz^{0.5}$ and set to 10–100 $nT/Hz^{0.5}$. The gradual reduction of the field noise at higher hard-axis bias fields is indicative of a better signal-to-noise ratio.

[Eq. (2)], we plot the magnetic field noise map (FNM) in Fig. 3(c). The color scale of the FNM (blue through dark red) has been set to 10–100 $nT/Hz^{0.5}$ to view properly the lowest magnetic field noise levels. As evident from the figure, vast regions of the map have field noise of over 100 $nT/Hz^{0.5}$. The MTJ sensitivity at these bias fields is almost vanishing [saturated free layer, Fig. 3(a)] with the corresponding voltage noise approaching a sensitivity-independent value [Fig. 3(b)]. Therefore, as the FNM clearly indicates, the biasing fields have to be carefully chosen in order to obtain the best sensing performance.

The most prominent result from the FNM is that the magnetic field noise is lower at higher values of the hard-axis bias fields. In other words, the magnetic field noise is not lowest when the field sensitivity is highest. Rather, it gets progressively lower at higher hard-axis bias fields. As the map shows, S_H approaches almost 10 $nT/Hz^{0.5}$ at the highest hard bias field (100 Oe), whereas it is about 35 $nT/Hz^{0.5}$ at regions where the sensitivity is maximum. The progressive lowering of the noise stems from the stability added to the free layer by the external hard-axis bias field.

The relation between S_H, as defined in Eq. (2), to the more fundamental magnetization noise is as follows:

$$S_H = (\delta V/V)/s = (1/sV)(\delta V/\delta H)(\delta H/\delta m)\delta m = \delta m/\chi. \quad (5)$$

Here δm represents the magnetization noise and χ is the magnetic susceptibility, dm/dH, of the MTJ free layer. Our results imply that the suppression in the magnetization noise of our MgO-MTJ samples is greater than the reduction in the susceptibility (or sensitivity) at higher hard-axis bias fields, leading to lower magnetic field noise values.

IV. CONCLUSIONS

In summary, we have analyzed the magnetic field sensitivity and low-frequency noise performance of MgO-based MTJs as a function of orthogonal easy- and hard-axis biasing fields. We have demonstrated that mapping these important benchmarks in a two-dimensional (2D) field provides us comprehensive information about the sensing characteristics of such devices, ranging from maximum sensitivity to its signal-to-noise ratio. Our MTJs showed sensitivities of over 1%/Oe only when a sufficiently strong hard-axis bias field was applied. The voltage noise map clearly indicates that the low-frequency $1/f$ noise scaled with the device sensitivity. The magnetic FNM revealed that the signal-to-noise ratio of MgO–MTJs progressively improved with increasing hard-axis bias field.

ACKNOWLEDGMENTS

This work was supported at Brown University by the National Science Foundation Grant No. DMR-0605966 and at Micro Magnetics, Inc., by the National Science Foundation Grant No. DMR-0522160.

[1] S. S. P. Parkin, C. Kaiser, A. Panchula, P. M. Rice, B. Hughes, M. Samant, and S. H. Yang, Nat. Mater. **3**, 862 (2004).
[2] S. Yuasa, T. Nagahama, A. Fukushima, Y. Suzuki, and K. J. Ando, Nat. Mater. **3**, 868 (2004).
[3] W. H. Butler, X.-G. Zhang, T. C. Schulthess, and J. M. MacLaren, Phys. Rev. B **63**, 054416 (2001).
[4] J. Mathon and A. Umerski, Phys. Rev. B **63**, 220403 (2001).
[5] S. Ingvarsson, G. Xiao, S. Parkin, W. Gallagher, G. Grinstein, and R. Koch, Phys. Rev. Lett. **85**, 3289 (2000).
[6] S. Ingvarsson, G. Xiao, R. A. Wanner, P. Trouilloud, Y. Lu, W. J. Gallagher, A. Marley, K. P. Roche, and S. S. P. Parkin, J. Appl. Phys. **85**, 5270 (1999).
[7] D. Mazumdar, X. Liu, B. D. Schrag, M. Carter, W. Shen, and G. Xiao, Appl. Phys. Lett. **91**, 033507 (2007).
[8] D. Mazumdar, X. Y. Liu, B. D. Schrag, W. Shen, M. Carter, and G. Xiao, J. Appl. Phys. **101**, 09B502 (2007).
[9] W. Shen, D. Mazumdar, X. Zou, X. Liu, B. D. Schrag, and G. Xiao, Appl. Phys. Lett. **88**, 182508 (2006).
[10] B. D. Schrag, A. Anguelouch, S. Ingvarsson, G. Xiao, Y. Lu, P. L. Trouilloud, A. Gupta, R. A. Wanner, W. J. Gallagher, P. M. Rice, and S. S. P. Parkin, Appl. Phys. Lett. **77**, 2373 (2000).
[11] C. Ren, X. Liu, B. D. Schrag, and G. Xiao, Phys. Rev. B **65**, 104405 (2004).